Transient model of mixed pole machines with eccentric reluctance rotor

A.L. Mohamadein, R.A. Hamdy and Ayman S. Abdel-Khalik
Electrical Eng. Dept., Faculty of Eng., Alexandria University, Alexandria, Egypt

This paper presents the modeling of Mixed Pole Machine (MPM) operating with eccentric rotors. The operation of a MPM machine with eccentric rotor positions creates asymmetrical air gap flux distribution that results in unbalanced magnetic pull. The winding function theory is used to calculate machine winding inductances as a function of rotor radial displacement. The effect of dynamic air-gap eccentricity on the inductances of salient rotor type has been discussed. Coupled magnetic circuits approach has been used to simulate the machine behavior under healthy and eccentric rotor conditions. Also, the paper presents the contribution of these inductances to the radial force production and how to use this machine in magnetic bearing applications.

تقدم هذه المقالة طريقة رياضية لتمثيل الماكينات ذات الأقطاب المختلطة ذات الأعضاء الدائرة اللامركزية والتى تتسبب فى عدم تماثل الفيض داخل الثغرة الهوائية. وتستخدم نظرية دالة اللفات لحساب محاثة ملفات الماكينة كدالة فى الإزاحة القطرية للعضو الدائر. وتم دراسة تأثير ديناميكية اللاتمركز للثغرة الهوائية على محاثة الملفات فى حالة العضو ذى الأقطاب البارزة. وتستخدم طريقة الدوائر المغناطيسية المتزاوجة لمحاكاة اداء الماكينة وذلك فى الحالة المركزية واللامركزية. كذلك تعرض المقالة لاسهام محاثة الملفات فى توليد القوى القطرية وكيفية استغلال هذه الماكينة فى تطبيقات كراسى التحميل المغناطيسية.

Keywords: Mixed pole machine, Radial force, Winding function, Magnetic bearings

1. Introduction

The idea of Mixed-Pole Machine (MPM) is to have two electrically connected and mechanically coupled machines in the same frame. The resulting new machine has combined characteristics from both machines.

The idea was firstly introduced from the so called “tandem connection” where two three-phase wound rotor induction machines are mechanically and electrically coupled. Mechanical coupling is done either directly or through gears, while connecting the rotor circuits provides the electric coupling. The method was launched in 1893 by Steimmetz and Gorge [1]. The idea of obtaining a single unit was implemented by Hunt in 1907 [1]. The Hunt motor represented a considerable advance over earlier machines; it comprised two windings on one stator and one rotor. The two stator windings share the same magnetic circuit.

Recently, the mixed pole machine is used for high-speed application as in machine tools, turbo-molecular pumps and high-speed flywheels. This is because this machine facilitates the application of magnetic bearings. A reluctance motor with magnetically combined radial force production is to be simulated in this paper. The motor is originally four-pole machines producing torque with revolving magnetic field. An additional two-pole winding is added in the stator slots forming a mixed pole machine. The four-pole magnetic field is intentionally unbalanced by the currents of the two-pole winding to produce radial force acting on the rotor [2].

The mixed pole machine presented in this paper comprises two stator windings with different number of pole pairs, namely P_1 and P_2, and reluctance rotor with $P_r = P_1+P_2$ saliencies, as shown in fig. 1. The two fields produced by the two-stator windings share the same magnetic circuit.

In this paper, the machine inductances are calculated as a function of rotor radial displacement and rotor angular position using winding function method [3]. Moreover, a mathematical dynamic model for mixed pole machine with eccentric rotor is proposed. The paper also investigates the contribution of these inductances to the radial force production. An expression for radial force is formulated as a function of winding currents as well

as the machine inductances. The machine radial forces are analyzed when the machine operates in the generating as well as motoring mode.

2. Determination of machine inductances

Fig. 1 shows the machine model of a bearing less motor with both four-pole and two-pole windings. These windings are wound in two phases to simplify the analysis. Three-phase windings model can be obtained by applying park's transformation. The perpendicular axes α and β are fixed in the stator. Φ is the angle along the inner surface of the stator. The two phases of the two-pole winding are N_A and N_B, while the two phases of the four-pole winding are N_a and N_b.

In cylindrical rotor, if the air-gap length g_o and the eccentric displacement are small enough compared to the rotor radius. The resultant air gap g_c can be written as [3]:

$$g_c = g_o - \alpha\cos(\phi) + \beta\sin(\phi), \tag{1}$$

where g_o is the air-gap length when the rotor center is aligned to the stator center. In normal operating conditions, the rotor center can be positioned to the stator center. This leads to the further assumption that the rotor displacements are small enough to g_o. Then, the inverse gap function can be written as:

$$g_c^{-1}(\phi_s) = \frac{1}{g_o}\left(1 + \frac{\alpha}{g_o}\cos(\phi) - \frac{\beta}{g_o}\sin(\phi)\right). \tag{2}$$

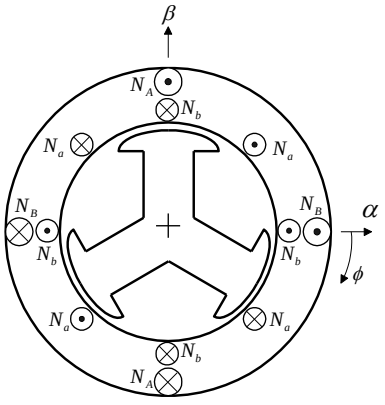

Fig. 1. 4/2 Poles MPM with reluctance rotor.

For salient pole rotor, the inverse air gap function is a function of pole arc ε. It can be formulated as:

$$g^{-1}(\theta_m,\phi) = \frac{1}{g_o}\left(1 + \frac{\alpha}{g_o}\cos(\phi) - \frac{\beta}{g_o}\sin(\phi)\right)$$
$$\frac{\pi}{P_r}(2(n-1)-\varepsilon) < \phi - \theta_m < \frac{\pi}{P_r}(2(n-1)+\varepsilon). \tag{3}$$

Where,

n is the 1,2, P_r (number of saliencies),

θ_m is the rotor angular position, and

ε is the rotor pole arc to the rotor pole pitch ratio.

Since, the inverse air gap function of a salient rotor is a function of the rotor angular position θ_m, the machine inductances are also function of the rotor angular position θ_m. The inductances are also functions of the rotor radial displacement. The orthogonal coordinates α and β are defined as shown in fig.1. Then, these inductance functions are represented by α, β and θ_m.

Various means can be used to calculate the machine inductances. This includes field theory, finite elements and various circuit approaches. A particular convenient approach called the winding functions. In this method, the inductances of the machine are calculated by the integral expression representing the placement of winding turns along the air gap periphery [4]. The method is particularly convenient for the analysis of unusual machines since it does not assume coil placement symmetry. Like most inductance calculations, the stator and rotor iron is assumed to have infinite permeability, saturation is neglected, stator surface is considered smooth and the slot effect is corrected by carter coefficient.

For sake of simplicity, the analysis for the considered machine is based on sinusoidal distribution of the stator main windings. The end effects, saturation and stator harmonics are also assumed negligible.

According to winding function theory, the mutual inductance between any two arbitrary windings i and j in any electric machine can be computed by the equation:

$$L_{ij}(\theta_m) = \mu_o.R.l\int_0^{2\pi} g^{-1}(\theta_m,\phi).N_i(\theta_m,\phi).N_j(\theta_m,\phi).d\phi\ , \tag{4}$$

Where,

μ_o	space permeability,
R	rotor radius,
l	rotor length,
θ_m	rotor angular position,
ϕ	angular position along the stator inner surface,
$g^{-1}(\theta_m, \Phi)$	the inverse gap function,
$N_i(\theta_m, \Phi)$	the winding function of winding i, and
$N_j(\theta_m, \Phi)$	the winding function of winding j.

The winding function of the winding represents the MMF distribution along the air gap for a unit current in the winding. If this winding is located on the stator, the winding function is only a function of the stator periphery angle ϕ while if the winding is located on the rotor the winding must be expressed as a function of both ϕ and the mechanical position of the rotor θ_m.

The windings distributions are shown in fig. 2. The windings distributions can be expressed, assuming sinusoidal distribution, as:

$$N_a(\phi) = N_1 \cos(2\phi), \quad (5)$$

$$N_b(\phi) = N_1 \sin(2\phi), \quad (6)$$

$$N_A(\phi) = N_2 \cos(\phi), \quad (7)$$

$$N_B(\phi) = N_2 \sin(\phi), \quad (8)$$

Where,

N_1 and N_2 are the equivalent number of turns per phase per pole.

The inverse air gap function for concentric and eccentric salient rotor is shown in fig. 3.

Substituting from eqs. (3) and (5-8) in eq. (4), the machine inductances can be calculated.

The machine self inductances for the 4-pole winding L_1 and the 2-pole winding L_2 are expressed in matrix form as,

$$[L_1] = \begin{bmatrix} L_{o1} & 0 \\ 0 & L_{o1} \end{bmatrix} + L_{m1}` \cdot \begin{bmatrix} \cos(3\theta_m) & \sin(3\theta_m) \\ \sin(3\theta_m) & -\cos(3\theta_m) \end{bmatrix} \cdot \begin{bmatrix} \alpha & -\beta \\ \beta & \alpha \end{bmatrix}, \quad (9)$$

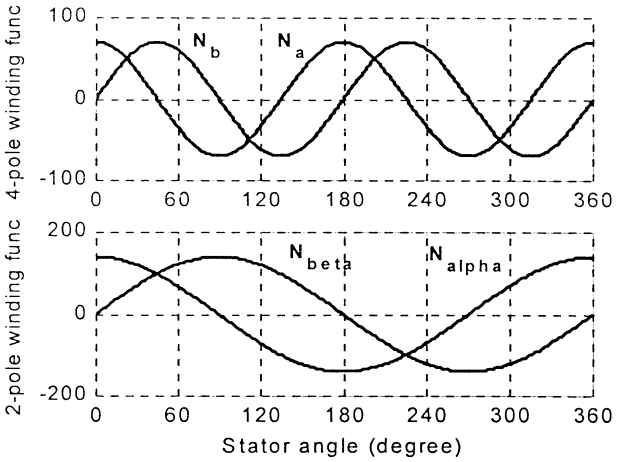

Fig. 2. Winding function for stator windings.

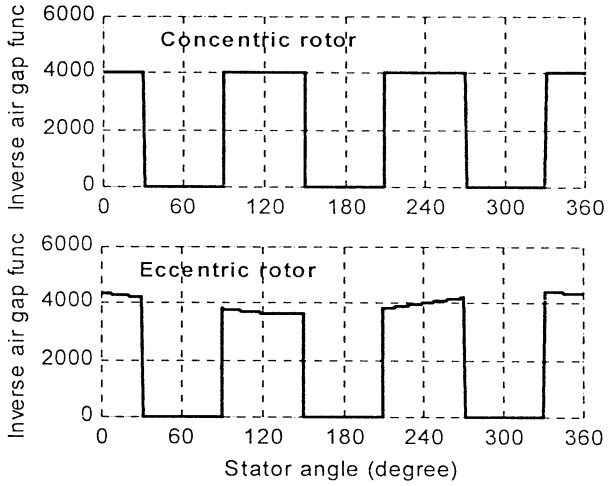

Fig. 3. Inverse air gap function.

$$[L_2] = \begin{bmatrix} L_{o2} & 0 \\ 0 & L_{o2} \end{bmatrix} + L_{m2}` \cdot \begin{bmatrix} \cos(3\theta_m) & \sin(3\theta_m) \\ \sin(3\theta_m) & -\cos(3\theta_m) \end{bmatrix} \cdot \begin{bmatrix} \alpha & \beta \\ -\beta & \alpha \end{bmatrix}. \quad (10)$$

The mutual inductances between the 4-pole and the 2-pole windings are expressed in matrix form as:

$$[M_{12}] = M_o` \cdot \begin{bmatrix} \alpha & \beta \\ -\beta & \alpha \end{bmatrix} + M_1 \cdot \begin{bmatrix} \cos(3\theta_m) & \sin(3\theta_m) \\ \sin(3\theta_m) & -\cos(3\theta_m) \end{bmatrix}. \quad (11)$$

Where,

$$L_{o1} = \frac{\mu_o.R.l.N_1^{\,2}\varepsilon\pi}{g},\quad L_{m1}` = \frac{\mu_o.R.l.N_1^{\,2}\sin(\varepsilon\pi)}{2g^2}$$

$$L_{o2} = \frac{\mu_o.R.l.N_2^{\,2}\varepsilon\pi}{g},\quad L_{m2}` = \frac{\mu_o.R.l.N_2^{\,2}\sin(\varepsilon\pi)}{2g^2}$$

$$M_1 = \frac{\mu_o.R.l.N_1\cdot N_2\cdot\sin(\varepsilon\pi)}{g},\quad M_o` = \frac{\mu_o.R.l.N_1\cdot N_2\cdot\varepsilon\pi}{2g^2}$$

Fig. 4 shows the inductance variations of the machine windings with respect to the rotor angular position where the rotor is positioned to the stator center. The self-inductances L_1 and L_2 are constant and independent of rotor angular position, which agree with eqs. (8) and (9) when α and β are set to zero. The mutual inductance M_{12} varies sinusoidally with rotor angular position.

As the rotor is displaced from the stator center, this results in sinusoidal components (L_{m1}, L_{m2}) that are superimposed on the dc component of the constant self-inductances components (L_{o1}, L_{o2}). Moreover, a dc offset M_o is superimposed on the sinusoidal variation of M_{12}. Fig. 5 shows the effect of eccentricity on the machine inductances.

From eqs. (9-11), the sinusoidal components (L_{m1}, L_{m2}) of the self inductances and the dc component (M_o) of the mutual inductance are expected to vary linearly with the rotor radial displacements α and β. However, these relations are not absolutely linear. On the other hand, the dc components (L_{o1}, L_{o2}) of the self-inductances and the sinusoidal component (M_1) of the mutual inductance are shown

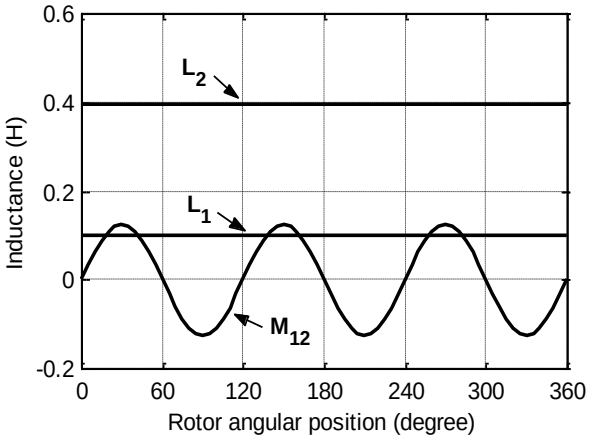

Fig. 4. Inductance variation with respect to the rotor angular position.

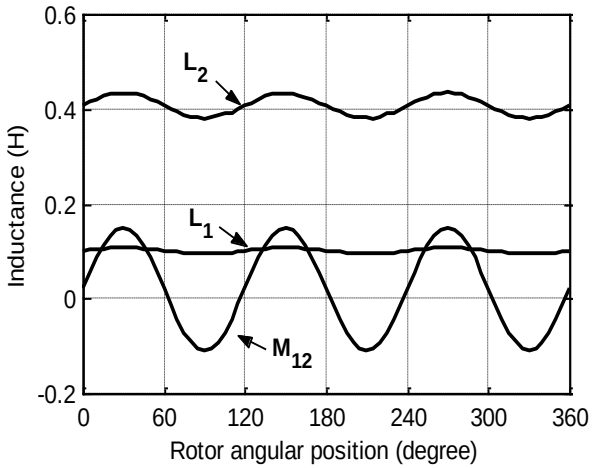

Fig. 5. Inductance variation with respect to the rotor angular position with rotor radial displacement $\alpha = 0.2g_o$.

to be constant and independent of rotor radial displacement. However, these components vary slightly as the rotor is displaced from the stator center. The actual variation of both sinusoidal and dc components of the self and mutual inductances with respect to the radial displacement in the α axis direction are illustrated in fig. 6. The horizontal axis a_n is the normalized rotor radial position with respect to the main air gap length g_o. All inductances become minimum when the rotor is positioned to the stator center ($a_n = 0$).

3. Radial force

The MPM radial force is calculated by the specific field energy method. This method is suitable for machines with different air gap configuration. The air gap can be constant or variable as in cylindrical or salient, concentric or eccentric rotors. The method is based on the well-known formula of force attraction F between infinitely permeable ferromagnetic surfaces with flux density B_g crossing the air gap surface area A between them. The air gap flux density B_g is given by,

$$B_g(\phi) = \mu_o F(\phi) g^{-1}(\phi)\cdot \tag{12}$$

For infinitesimal small air-gap area dA the radial force is given by,

$$dF = \frac{B_g^{\,2}}{2\mu_o}\,dA\cdot \tag{13}$$

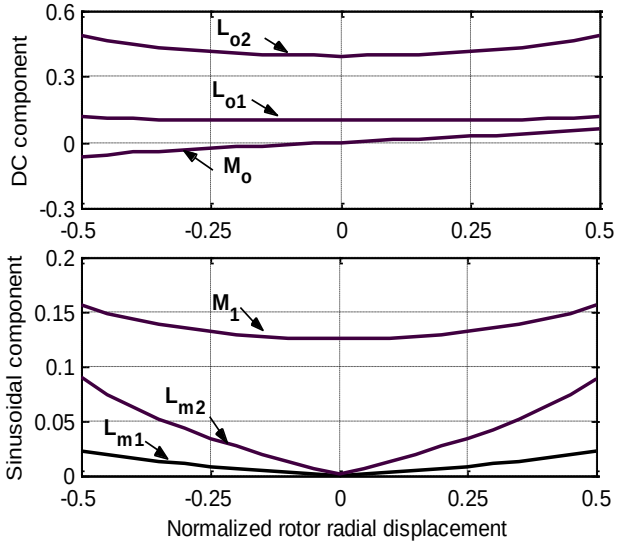

Fig. 6. Variation of inductance components with respect to the rotor radial displacement.

Where,

$$dA = R \cdot l \cdot d\phi .$$

Hence, the horizontal and vertical radial force components dF_x and dF_y acting on dA can be formulated as:

$$dF_x = \frac{B_g{}^2}{2\mu_o} cos(\phi) \cdot dA, \tag{14}$$

$$dF_y = \frac{B_g{}^2}{2\mu_o} sin(\phi) \cdot dA. \tag{15}$$

The radial force components F_x and F_y are then determined by the integration over the total air gap surface $(0 \le \phi \le 2\pi)$.

$$F_x = \int_0^{2\pi} \frac{B_g{}^2}{2\mu_o} cos(\phi) \cdot dA, \tag{16}$$

$$F_y = \int_0^{2\pi} \frac{B_g{}^2}{2\mu_o} sin(\phi) \cdot dA. \tag{17}$$

Assuming that the fields produced by the two stator windings are sinusoidally distributed and given by,

$$F_1(\phi, t) = F_{m1} cos(\omega_1 t - 2\phi - \gamma_1), \tag{18}$$

$$F_2(\phi, t) = F_{m2} cos(\omega_2 t - \phi - \gamma_2), \tag{19}$$

Where;
ω_1 and ω_2 are the excitation frequencies of the two windings,
$\gamma_1$and γ_2 are the phase shift of the two MMFs at time zero, and
F_{m1} and F_{m2} are the MMF amplitudes.

The stator total MMF is given by:

$$\bar{F} = \bar{F_1} + \bar{F_2}. \tag{20}$$

Hence, the total MMF can be written in complex form as:

$$\bar{F} = F_m e^{j\theta}, \tag{21}$$

where

$$F_m = \sqrt{F_{m1}^2 + F_{m2}{}^2 + 2F_{m1}F_{m2} cos((\omega_1 - \omega_2) \cdot t - \cdot\phi - (\gamma_1 - \gamma_2))} \tag{22}$$

$$\theta = sin^{-1}\left(\frac{F_{m1}}{F_m} \cdot sin((\omega_1 - \omega_2) \cdot t - \cdot\phi - (\gamma_1 - \gamma_2)) \right) + \omega_2 t - \phi - \gamma_2. \tag{23}$$

Eqs. (22) and (23) state that the stator total MMF is a space phasor with variable magnitude F_m and variable phase θ. Also, the envelope of the total MMF is described by the peaks of the total MMF patterns, which is given by eq. (22).

If the excitation frequencies ω_1 and ω_2 are equal, then the envelope of the MMF wave will be stationary. The stationary axis direction is determined by the phase shift ($\gamma_1 - \gamma_2$) as shown in fig. 7. This angle can be controlled by controlling the current in one or both of the stator windings. However, the value of maximum MMF (F_m) can be controlled by the amplitude of the two-stator windings current. This develops the idea of magnetic bearings using the MPM. Fig. 8 illustrates the field distribution for $\gamma_1 - \gamma_2 = 0$, $\pi/4$, $\pi/2$ and $3\pi/4$.

4. Machine dynamic equations

In this section, the machine dynamic model is produced [7]. Also, an expression of the machine radial forces as a function in winding currents is introduced.

First, the following definitions are introduced:

$$[\lambda_1]=\begin{bmatrix}\lambda_a\\ \lambda_b\end{bmatrix},\ [\lambda_2]=\begin{bmatrix}\lambda_A\\ \lambda_B\end{bmatrix},\ [i_1]=\begin{bmatrix}i_a\\ i_b\end{bmatrix},\ [i_2]=\begin{bmatrix}i_A\\ i_B\end{bmatrix}$$

Hence,

$$\begin{bmatrix}\lambda_A\\ \lambda_B\end{bmatrix}=\begin{bmatrix}L_{o2} & 0\\ 0 & L_{o2}\end{bmatrix}\cdot\begin{bmatrix}i_A\\ i_B\end{bmatrix}$$
$$+L_{m2}`\cdot\begin{bmatrix}\cos(3\theta_m) & \sin(3\theta_m)\\ \sin(3\theta_m) & -\cos(3\theta_m)\end{bmatrix}\cdot\begin{bmatrix}\alpha & \beta\\ -\beta & \alpha\end{bmatrix}\cdot\begin{bmatrix}i_A\\ i_B\end{bmatrix}$$
$$+M_o\cdot\begin{bmatrix}\cos(3\theta_m) & \sin(3\theta_m)\\ \sin(3\theta_m) & -\cos(3\theta_m)\end{bmatrix}\cdot\begin{bmatrix}i_a\\ i_b\end{bmatrix}$$
$$+M_1`\cdot\begin{bmatrix}\alpha & -\beta\\ \beta & \alpha\end{bmatrix}\cdot\begin{bmatrix}i_a\\ i_b\end{bmatrix} \qquad (24)$$

$$\begin{bmatrix}\lambda_a\\ \lambda_b\end{bmatrix}=\begin{bmatrix}L_{o1} & 0\\ 0 & L_{o1}\end{bmatrix}\cdot\begin{bmatrix}i_a\\ i_b\end{bmatrix}$$
$$+L_{m1}`\cdot\begin{bmatrix}\cos(3\theta_m) & \sin(3\theta_m)\\ \sin(3\theta_m) & -\cos(3\theta_m)\end{bmatrix}\cdot\begin{bmatrix}\alpha & -\beta\\ \beta & \alpha\end{bmatrix}\cdot\begin{bmatrix}i_a\\ i_b\end{bmatrix}$$
$$+M_o\cdot\begin{bmatrix}\cos(3\theta_m) & \sin(3\theta_m)\\ \sin(3\theta_m) & -\cos(3\theta_m)\end{bmatrix}\cdot\begin{bmatrix}i_A\\ i_B\end{bmatrix}$$
$$+M_1`\cdot\begin{bmatrix}\alpha & \beta\\ -\beta & \alpha\end{bmatrix}\cdot\begin{bmatrix}i_A\\ i_B\end{bmatrix}. \qquad (25)$$

Now apply the definition of space phasor flux linkage to flux linkage as follows:

$$\overline{\lambda_1}=\lambda_a+j\lambda_b, \qquad (26)$$

$$\overline{\lambda_2}=\lambda_A+j\lambda_B. \qquad (27)$$

Hence,

$$\overline{\lambda_1}=[1\quad j]\cdot\begin{bmatrix}\lambda_a\\ \lambda_b\end{bmatrix},\ \overline{\lambda_2}=[1\quad j]\cdot\begin{bmatrix}\lambda_A\\ \lambda_B\end{bmatrix}, \qquad (28)$$

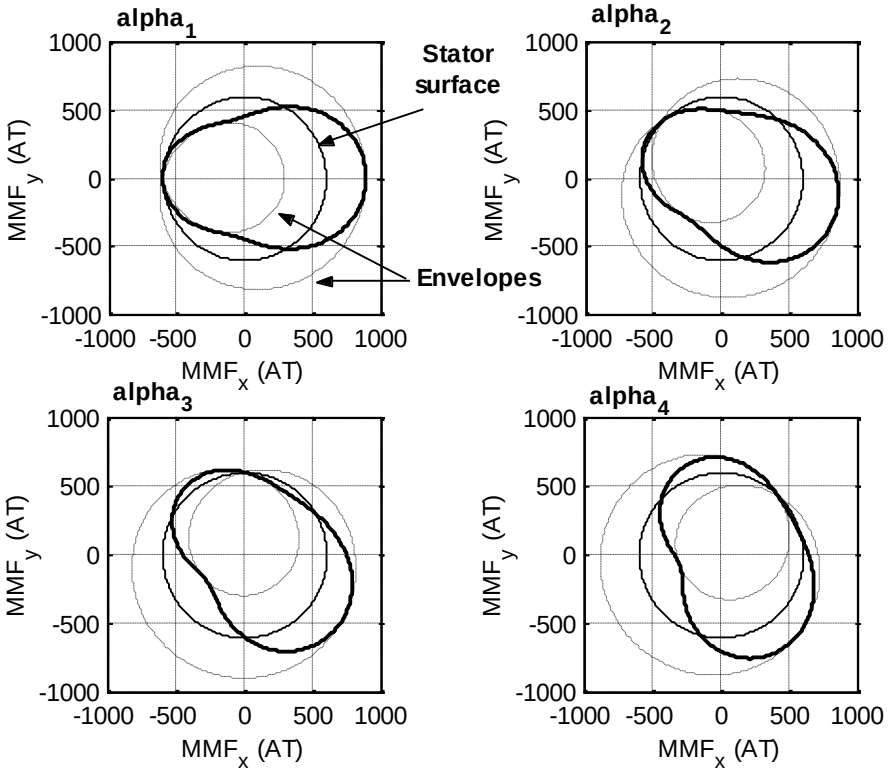

Fig. 7. Stator MMF distribution at different phase shift angles.

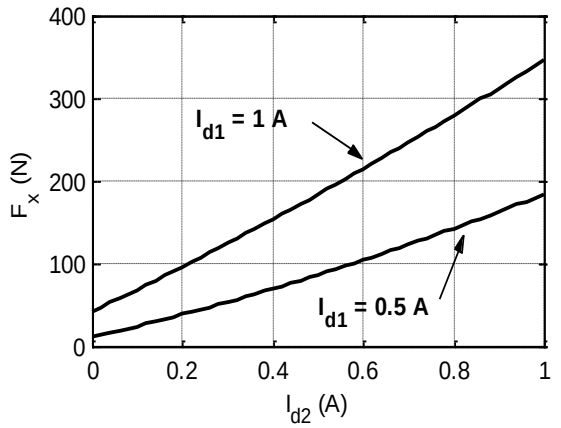

Fig. 8. Radial force variation with windings currents magnitude.

$$\overline{\lambda_1} = L_{o1}\overline{i_1} + L_{m1}(\alpha - j\beta)\cdot e^{3j\theta_m}\,\overline{i_1}^{*} + M_1\cdot\overline{i_2}^{*}\cdot e^{3j\theta_m} + M_o^{'}\cdot(\alpha - j\beta)\cdot\overline{i_2} \quad (29)$$

By multiplying both sides of eq. (29) by $e^{-j2\theta_m}$, yields:

$$\overline{\lambda_1}e^{-j2\theta_m} = L_{o1}\overline{i_1}e^{-j2\theta_m} + L_{m1}(\alpha - j\beta)\cdot e^{j\theta_m}\,\overline{i_1}^{*} + M_1\cdot\overline{i_2}^{*}\cdot e^{j\theta_m} + M_o^{'}\cdot(\alpha - j\beta)\cdot\overline{i_2}\cdot e^{-2j\theta_m}. \quad (30)$$

Similarly,

$$\overline{\lambda_2} = L_{o2}\overline{I_2} + L_{m2}(\alpha + j\beta)\cdot e^{3j\theta_m}\,\overline{I_2}^{*} + M_1\cdot\overline{i_1}^{*}\cdot e^{3j\theta_m} + M_o^{'}\cdot(\alpha - j\beta)\cdot\overline{i_1}. \quad (31)$$

By multiplying both sides of eq. (31) by $e^{-j\theta_m}$, yields:

$$\overline{\lambda_2}e^{-j\theta_m} = L_{o2}\overline{i_2}e^{-j\theta_m} + L_{m2}(\alpha + j\beta)\cdot e^{2j\theta_m}\,\overline{i_2}^{*} + M_1\cdot\overline{i_1}^{*}\cdot e^{2j\theta_m} + M_o^{'}\cdot(\alpha + j\beta)\cdot\overline{i_1}\cdot e^{-j\theta_m}. \quad (32)$$

Now define,

$$\overline{\lambda_{1f}} = \overline{\lambda_1}e^{-j2\theta_m},\ \overline{\lambda_{2f}} = \overline{\lambda_2}e^{-j\theta_m}$$
$$\overline{i_{1f}} = \overline{i_1}e^{-j2\theta_m},\ \overline{i_{2f}} = \overline{i_2}e^{-j\theta_m}. \quad (33)$$

Notice that $\overline{\lambda_{1f}}$, $\overline{i_{1f}}$ and $\overline{i_{2f}}$ are complex quantities in rotor coordinates aligned with the rotor *d*- axis. Therefore,

$$\overline{\lambda_{1f}} = L_{o1}\overline{i_{1f}} + L_{m1}(\alpha - j\beta)\cdot e^{-j\theta_m}\,\overline{i_{1f}}^{*} + M_1\cdot\overline{i_{2f}}^{*} + M_o^{'}(\alpha - j\beta)\cdot e^{-j\theta_m}\overline{i_{2f}}. \quad (34)$$

Define,

$$\begin{bmatrix} x \\ y \end{bmatrix} = \begin{bmatrix} \cos(\theta_m) & -\sin(\theta_m) \\ \sin(\theta_m) & \cos(\theta_m) \end{bmatrix}\cdot\begin{bmatrix} \alpha \\ \beta \end{bmatrix}. \quad (35)$$

Where x and y are the corresponding rotor radial displacement in rotor reference frame. Therefore,

$$(x - jy) = (\alpha - j\beta)\cdot e^{-j\theta_m}, \quad (36)$$

$$(x + jy) = (\alpha + j\beta)\cdot e^{j\theta_m}. \quad (37)$$

Hence,

$$\overline{\lambda_{1f}} = L_{o1}\overline{i_{1f}} + L_{m1}(x - jy)\cdot\overline{i_{1f}}^{*} + M_1\cdot\overline{i_{2f}}^{*} + M_o^{'}(x - jy)\cdot\overline{i_{2f}}. \quad (38)$$

Similarly,

$$\overline{\lambda_{2f}} = L_{o2}\overline{i_{2f}} + L_{m2}(\alpha + j\beta)\cdot e^{j\theta_m}\,\overline{i_{2f}}^{*} + M_1\cdot\overline{i_{1f}}^{*} + M_o^{'}(\alpha + j\beta)\cdot e^{j\theta_m}\overline{i_{1f}}, \quad (39)$$

$$\overline{\lambda_{2f}} = L_{o2}\overline{i_{2f}} + L_{m2}(x + jy)\cdot\overline{i_{2f}}^{*} + M_1\cdot\overline{i_{1f}}^{*} + M_o^{'}(x + jy)\cdot\overline{i_{1f}}. \quad (40)$$

Next, the voltage equations of the two windings are:

$$v_a = R_1 i_a + \frac{d\lambda_a}{dt},\ v_b = R_1 i_b + \frac{d\lambda_b}{dt}, \quad (41)$$

$$v_A = R_2 i_A + \frac{d\lambda_A}{dt},\ v_B = R_2 i_B + \frac{d\lambda_B}{dt}, \quad (42)$$

Now using the voltage equations on conjunction with definition of space phasor yields,

$$\overline{v}_{1f}e^{-2j\theta_m} = R_1\overline{i}_{1f}e^{-j2\theta_m} + \frac{d}{dt}\left(\overline{\lambda}_{1f}e^{-2j\theta_m}\right), \quad (43)$$

which takes the following final form:

$$\bar{v}_{1f} = R_1 \bar{i}_{1f} + \frac{d\bar{\lambda}_{1f}}{dt} + 2j\omega_m \bar{\lambda}_{1f} . \quad (44)$$

Similarly,

$$\bar{v}_{2f} = R_2 \bar{i}_{2f} + \frac{d\bar{\lambda}_{2f}}{dt} + j\omega_m \bar{\lambda}_{2f} . \quad (45)$$

Eqs. (43) and (44) are the space phasor equations in a system of coordinates rotating at speed ω_m (rotor speed).

The *dq*- model of the machine may now be developed by resolving the stator complex quantities along the *d*-axis and the *q*-axis; that is,

$$\bar{i}_{1f} = i_{d1} + j i_{q1}, \quad (46)$$

$$\bar{i}_{2f} = i_{d2} + j i_{q2} . \quad (47)$$

Similar expressions for voltages, flux linkage can be defined.

Consequently, the dq components of the machine flux linkage for both windings are expressed in matrix form as:

$$\begin{bmatrix} \lambda_{d1} \\ \lambda_{q1} \\ \lambda_{d2} \\ \lambda_{q2} \end{bmatrix} = \begin{bmatrix} L_{o1} + L_{m1}\grave{}x & -L_{m1}\grave{}y & M_1 + M_o\grave{}x & M_o\grave{}y \\ -L_{m1}\grave{}y & L_{o1} - L_{m1}\grave{}x & -M_o\grave{}y & -M_1 + M_o\grave{}x \\ M_1 + M_o\grave{}x & -M_o\grave{}y & L_{o2} + L_{m2}\grave{}x & L_{m2}\grave{}y \\ M_o\grave{}y & -M_1 + M_o\grave{}x & L_{m2}\grave{}y & L_{o2} + L_{m2}\grave{}x \end{bmatrix} . \begin{bmatrix} i_{d1} \\ i_{q1} \\ i_{d2} \\ i_{q2} \end{bmatrix} . \quad (48)$$

With the decomposition defined by eqs. (46-47), the voltage eqs. (44,45) may be expressed as two components:

$$v_{d1} = R_1 i_{d1} + p\lambda_{d1} - 2\omega_m \lambda_{q1}, \quad (49)$$

$$v_{q1} = R_1 i_{q1} + p\lambda_{q1} + 2\omega_m \lambda_{d1} , \quad (50)$$

$$v_{d2} = R_2 i_{d2} + p\lambda_{d2} - \omega_m \lambda_{q2} , \quad (51)$$

$$v_{q2} = R_2 i_{q2} + p\lambda_{q2} + \omega_m \lambda_{d2} . \quad (52)$$

The magnetic energy W_m stored in the windings can be written as:

$$W_m = \begin{bmatrix} i_{d1} & i_{q1} & i_{d2} & i_{q2} \end{bmatrix} . \begin{bmatrix} L_{o1} + L_{m1}\grave{}x & -L_{m1}\grave{}y & M_1 + M_o\grave{}x & M_o\grave{}y \\ -L_{m1}\grave{}y & L_{o1} - L_{m1}\grave{}x & -M_o\grave{}y & -M_1 + M_o\grave{}x \\ M_1 + M_o\grave{}x & -M_o\grave{}y & L_{o2} + L_{m2}\grave{}x & L_{m2}\grave{}y \\ M_o\grave{}y & -M_1 + M_o\grave{}x & L_{m2}\grave{}y & L_{o2} + L_{m2}\grave{}x \end{bmatrix} . \begin{bmatrix} i_{d1} \\ i_{q1} \\ i_{d2} \\ i_{q2} \end{bmatrix} . \quad (53)$$

The components F_x and F_y in the *x*- and *y*-direction in the produced radial forces, assuming linear magnetic circuit, can be written as:

$$F_x = \frac{\partial W_m}{\partial x} , \; F_y = \frac{\partial W_m}{\partial y} , \quad (54)$$

$$F_x = \frac{1}{2}[i]^t \frac{\partial[L]}{\partial x}[i], F_y = \frac{1}{2}[i]^t \frac{\partial[L]}{\partial y}[i]. \quad (55)$$

Substituting from eq. (53) in eq. (54), the *x*-*y* components of the radial force can be formulated as:

$$\begin{aligned} F_x = {} & \frac{1}{2} L_{m1}\grave{}\left(i_{d1}{}^2 - i_{q1}{}^2\right) \\ & + \frac{1}{2} L_{m2}\grave{}\left(i_{d2}{}^2 - i_{q2}{}^2\right) \\ & + M_o{}'\left(i_{d1} i_{d2} + i_{q1} i_{q2}\right), \end{aligned} \quad (56)$$

$$F_y = -L_{m1}{}' i_{d1} i_{q1} + L_{m2}{}' i_{d2} i_{q2} + M_o{}'\left(i_{d1} i_{q2} - i_{q1} i_{d2}\right) \quad (57)$$

From the transformation defined in eq (33), the *dq* components of the winding current is

the rotational frame can be obtained from the following transformation matrix:

$$\begin{bmatrix} i_{d1} \\ i_{q1} \end{bmatrix} = \begin{bmatrix} \cos(2\theta_m) & \sin(2\theta_m) \\ -\sin(2\theta_m) & \cos(2\theta_m) \end{bmatrix} \cdot \begin{bmatrix} i_a \\ i_b \end{bmatrix}, \quad (58)$$

$$\begin{bmatrix} i_{d2} \\ i_{q2} \end{bmatrix} = \begin{bmatrix} \cos(\theta_m) & \sin(\theta_m) \\ -\sin(\theta_m) & \cos(\theta_m) \end{bmatrix} \cdot \begin{bmatrix} i_A \\ i_B \end{bmatrix}. \quad (59)$$

Also, the radial force components F_α and F_β in the stationary coordinates α and β are given by:

$$\begin{bmatrix} F_\alpha \\ F_\beta \end{bmatrix} = \begin{bmatrix} \cos(\theta_m) & \sin(\theta_m) \\ -\sin(\theta_m) & \cos(\theta_m) \end{bmatrix} \cdot \begin{bmatrix} F_x \\ F_y \end{bmatrix}. \quad (60)$$

Examination of eqs. (56) and (57) reveals that both components of radial force F_x and F_y consist of three components, 4-pole winding current component, 2-pole winding component and component resulting from the interaction between two windings.

To discuss the effect of windings currents on the radial forces, the following case is to be simulated. The motor speed is set to zero. Phase a current i_a is kept constant while the phase *A* current i_A is varied. Fig .8 illustrates the variation of radial force with respect to current i_{d2} at two different values of i_{d1} (0.5A and 1A). It should be noted that, when i_{d2} is zero the radial force produced is due to the component generated by the 4-pole winding current, as mentioned previously. It is also noted that, the relation actually is not exactly linear.

5. Simulation results

In this section, the machine is simulated in different modes of operation to investigate the effect of operating conditions on radial forces.

5.1. Singly fed operation

In this mode, the 4-pole stator is connected to 60V, 50Hz AC supply and the 2-pole stator is short-circuited. In this case, the machine behaves as a conventional slip ring induction motor having a synchronous speed of ω_1/P_r. It is clear that this connection has a synchronous speed of 1000 r.p.m as shown in fig. 9. During run up, the stator 2 winding frequency decreases. This reduction should agree with the frequency relation $\omega_m = (\omega_1 + \omega_2)/(P_1+P_2)$ [7]. At no load, the magnitudes of stator 2 current and frequency are zero. The motor is loaded with 0.2 N.m load torque at 0.6 sec. The motor speed decreases to 940 r.p.m. Also, the 2-pole stator frequency equals to the slip frequency, as in the conventional induction motor. The *dq* components in rotor reference frame of the currents for both windings are shown in fig. 10.

The components of the radial force and the total radial force are shown in figs. 11 and 12. From fig. 12, it is noted that the radial force profile at steady state is a centered circle around origin.

5.2. Doubly fed operation

When the MPM is doubly fed, it operates at a synchronous speed given by $\omega_m=(\omega_1+\omega_2)/(P_1+P_2)$ [7]. Asynchronous operation may exist during doubly fed starting or loss of synchronism. In asynchronous mode each winding has two different frequencies and therefore four frequencies exist. As an example of doubly fed asynchronous operation is the starting up response. In this case 4-pole stator is connected to 60V, 50Hz AC supply and two lines of the 2-pole stator winding are connected to 40V DC supply (20V/phase). Fig. 13 shows that the machine starts up and self synchronizes at 1000 r.p.m. The response is similar to the starting up response of synchronous machine. Also, fig. 14 illustrates the current *dq* components in rotor reference

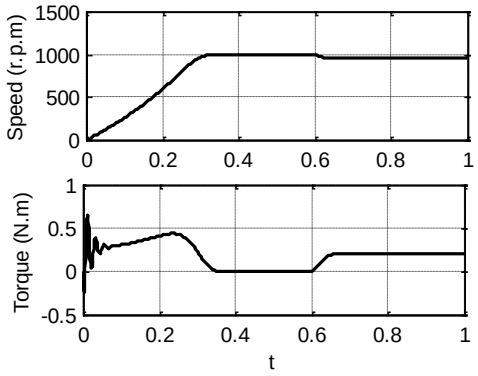

Fig. 9. Machine speed and torque for singly fed operation.

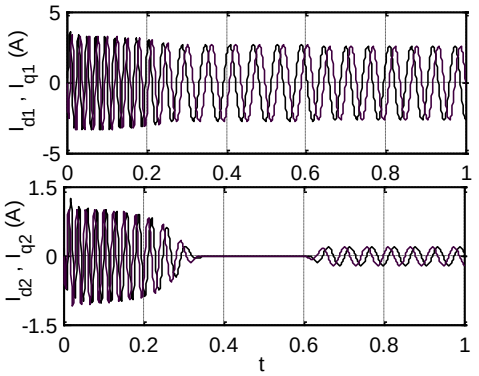

Fig. 10. *dq* components of machine currents.

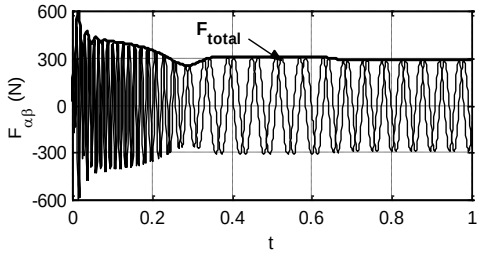

Fig. 11. Radial force with time.

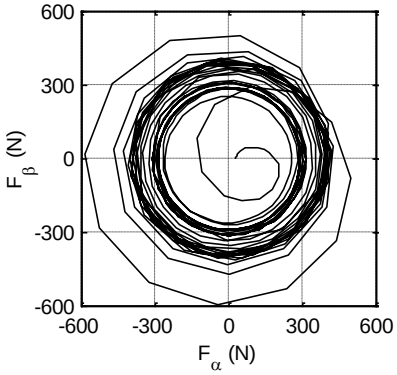

Fig. 12. *a-β* components of radial force.

frame for both windings currents. The machine is loaded by 0.5 N.m at 1 sec. The machine response to this load sudden application is shown in fig. 13. The speed curve shows that the machine returns to synchronism after a small transient period. The components of the radial force and the total radial force are shown in figs 15 and 16. From fig. 16, it is noted that the radial force profile at steady state is a circle centered on the origin.

5.3. Generation mode

For a constant prime mover speed, a dc excitation voltage applied to the control

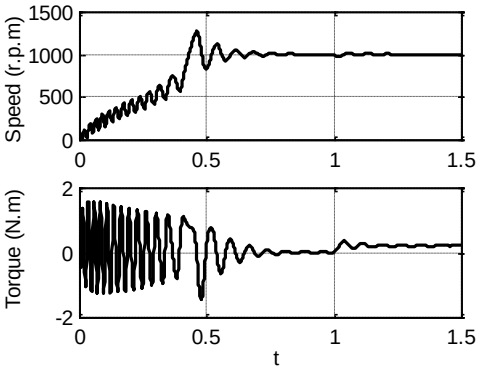

Fig. 13. Machine speed and torque for doubly fed operation.

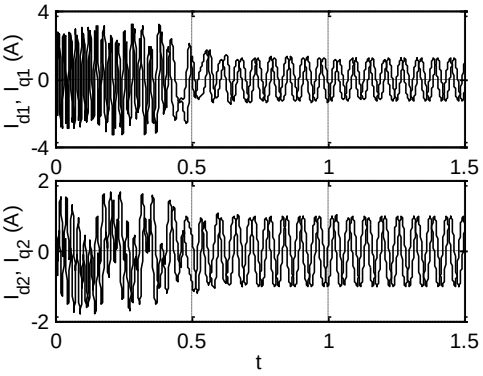

Fig. 14. *dq* components of machine currents.

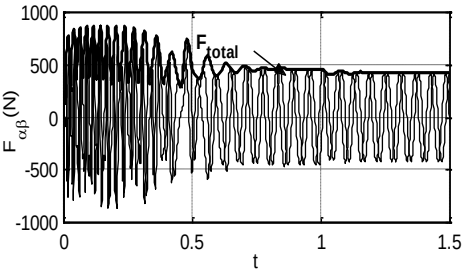

Fig. 15. Radial force with time.

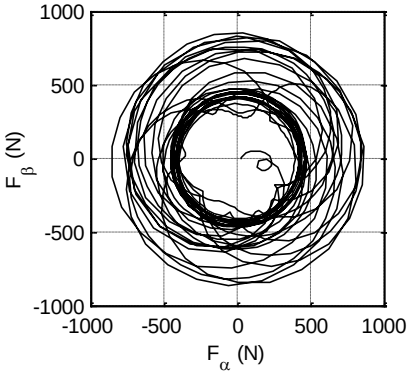

Fig. 16. *a-β* components of radial force.

winding (2-pole winding) generates power in the 4-pole winding. The voltage magnitude of the 4-pole winding is controlled by the dc excitation voltage applied to the 2-pole winding. However, the frequency of the 4-pole winding voltage is determined by the prime mover speed as in conventional synchronous generator. As an example, it is assumed that the machine is driven at constant speed of 1000 r.p.m. The 2-pole winding is excited by 40V dc between two lines (20V /phase). Under this condition the voltage build up response across the 4-pole winding is shown in fig. 17. The 4-pole winding is connected to resistive load of 200 Ω at 0.3 sec. Loading causes the generated terminal voltage V_1 to decrease. Fig. 18 illustrates the *dq* components in rotor reference frame for the windings currents. The components of the radial forces and the total radial force are shown in figs. 19 and 20. From fig. 19, it is noted that the radial force profile at steady state is circle centered on the origin.

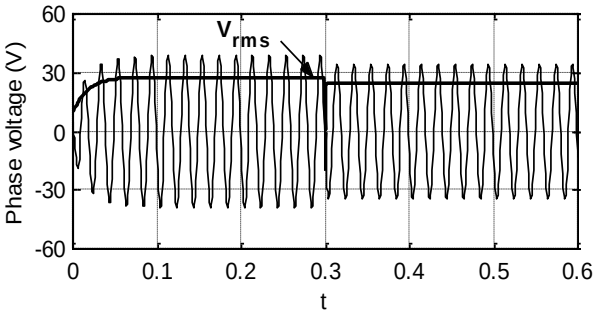

Fig. 17. Voltage across the 4-pole winding.

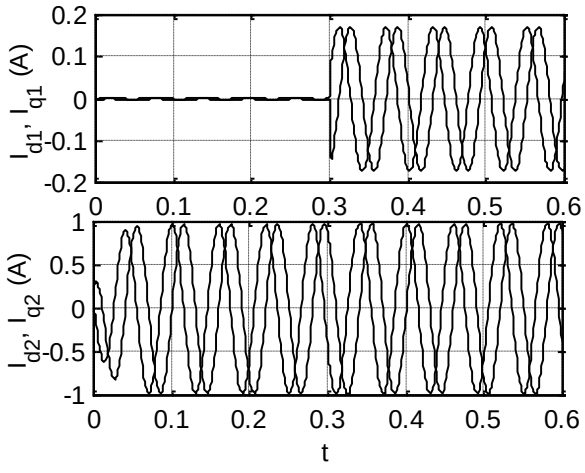

Fig. 18. *dq* components of machine currents.

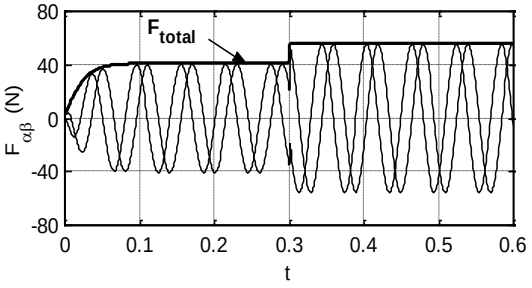

Fig. 19. Radial force with time.

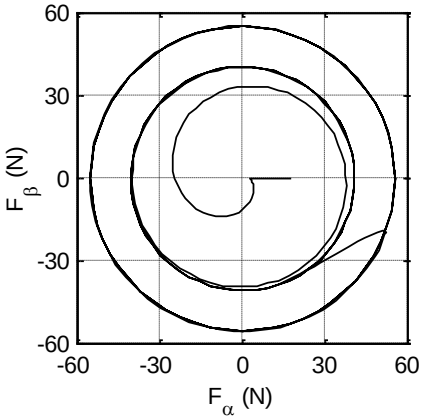

Fig. 20. *a-β* components of radial force.

6. Conclusions

This paper presents the modeling of Mixed Pole Machine (MPM) under eccentric rotors. Expressions for the machine inductance variations with respect to rotor radial displacement and rotor angular position were formulated using winding function method. A dynamic model for the machine as a function of rotor eccentricity was produced. An expression of radial force as a function of winding currents and inductances was produced. Simulation study was carried out to investigate the machine radial forces when the machine operates in both motoring and generating modes.

Appendix

MPM machine data:

Rated Power	250 W
4-pole winding voltage	60 V
4-pole winding current	2.1 A
4-pole winding frequency	50 Hz
Control 2-pole winding voltage	0 to 120 V

2-pole winding current	1.2 A
2-pole winding frequency	-50 to 50 Hz
Number of turns per phase per pole:	
2-pole winding	140 turn
4-pole winding	70 turn
Machine dimensions:	
Rotor radius	3 cm
Rotor length	8.5 cm
Air gap length	0.375 mm

Machine Parameters:
4-pole stator:
R_1 = 22.3 Ω, L_1 = 0.1084 H
2-pole stator:
R_2 = 23.43 Ω, L_2 = 0.4072 H
Mutual Inductance between two stators:
M_{12} = 0.115 H
L_{m1}` = 83.74 H/m
L_{m2}` = 334.97 H/m
M_o` = 263.08 H/m

References

[1] A.R.W. Broadway, L. Burbridge, "Self-Cascaded Machine: a Low-Speed Motor or High-Frequency Brushless Alternator", Proc., IEE, Vol. 117 (7), pp. 1277-1290 (1970).

[2] Akira Chiba, M. Azizur Rahman and Tadashi Fuako "Radial Force in a Bearingless Reluctance Motor", IEEE Trans on Magnetics, VOL. 27 (2), pp. 786-790 (1991).

[3] A. Chiba, T. Deido, T. Fukao and M.A. Rahman "An Analysis of Bearingless ac Motors", IEEE Trans on Energy Conversion, Vol. 9 (1) pp. 61-67 (1994).

[4] L. Xu, F. Liang and T.A. Lipo "Transient Model of a Doubly Excited Reluctance Motor", Ieee Trans on Energy Conversion, Vol. 6 (1) pp. 126-133 (1991).

[5] Masahide Ooshima, Akira Chiba, Tadashi Fuako and M. Azizur Rahman "Design and Analysis of Permanent Magnet-Type Bearingless Motors", IEEE Trans on Industrial Electronics, Vol. 43 (2), pp. 292-299 (1996).

[6] P.C. Krause, Analysis of Electric Machinary, McGraw-Hill (1986).

[7] M. Mustafa El_Daba Mixed Pole Machine, Ph.D Thesis, Alexandria University, Egypt (2001).

Received May 10, 2004
Accepted June 20, 2004